

Cu-Doped TiO₂ Nanopowders Synthesized by Sonochemical-assisted Process (Serbuk Nano Cu-terdop TiO₂ Disediakan Melalui Proses Sonokimia Terbantu)

NARONGDET WONGPISUTPAISAN*, NARATIP VITTAYAKORN,
ANUCHA RUANGPHANIT & WISANU PECHARAPA

ABSTRACT

Cu-doped TiO₂ nanopowders were prepared by sonochemical-assisted process via a precursor solution of titanium isopropoxide, copper nitrate trihydrate and sodium hydroxide in the presence of polyvinyl alcohol in combination with calcinations process. The as-synthesized products were calcined at various temperatures ranging from 500-1000°C. The physical microstructures, morphologies and chemical bonding of as-calcined nanopowders were characterized by X-ray diffraction, scanning electron microscopy and Fourier transform infrared spectroscopy. It was noted that the crystallization, structure and size of the powders were strongly dependent on calcinations temperature. Their optical absorption properties were investigated and the results suggested that Cu dopant could significantly improve the optical absorption properties of TiO₂.

Keywords: Cu-doped TiO₂; nanopowders; sonochemical-assisted process

ABSTRAK

Serbuk nano Cu-terdop TiO₂ telah disediakan melalui proses sonokimia terbantu melalui penggunaan larutan titanium isopropoksida, kuprum nitrat trihidrat dan natrium hidroksida dengan kehadiran polivinil alkohol berserta gabungan proses pemanasan. Produk yang tersintesis dipanaskan pada suhu yang berbeza, antara 500-1000°C. Mikrostruktur, morfologi dan ikatan kimia serbuk nano yang dipanaskan telah dicirikan menggunakan pembelauan sinar-X, mikroskop elektron imbasan dan spektroskopi transformasi Fourier inframerah. Penghabluran, struktur dan saiz serbuk sangat bergantung kepada suhu pemanasan. Sifat penyerapan optik telah diselidik dan hasilnya menunjukkan bahawa Cu terdop dapat meningkatkan sifat penyerapan optik TiO₂ secara signifikan.

Kata kunci: Cu-terdop TiO₂; proses sonokimia terbantu; serbuk nano

INTRODUCTION

In the past few decades, TiO₂ has been recognized as one of the most widely used metal oxide semiconductors due to its exceptional properties such as wide bandgap (3.2 eV), strong ultraviolet absorptivity, good photocatalytic activity, high energy conversion efficiency, non-toxicity and long-term chemical stability (Jitputti et al. 2007; Wang et al. 2009). The wide applications of titanium oxide (TiO₂) in the fields of photocatalysis, gas sensors, pigments, photovoltaic cells and semiconductors have made this material the focus of many interesting projects (Deng et al. 2011; Viana et al. 2010; Yu et al. 2011).

Owing it to the increasing interest in the application of nanosize TiO₂ in different fields, a large number of literatures on TiO₂ dealing with the synthesis, properties and applications of the different nanosize and structures TiO₂ crystalline forms have been reported. Low-dimensional TiO₂-related nanomaterials could be synthesized by various methods including, electrospinning (Li & Xia 2003), hydrogen treatment (Yoo et al. 2004), anodic oxidation of a titanium sheet (Gong et al. 2001), hydrothermal process (Kasuga et al.

1999), co-precipitation process (Viana et al. 2010) and sonochemical process (Arami et al. 2001).

A sonochemical method has been proven as a versatile and promising technique for generating a variety of novel materials metal oxide. Recently, it has been reported that the fundamental properties of TiO₂ can be enhanced by many techniques such as doping with variety elements and composited with compatible materials. There are a number of publications reported on the synthesis and characterization of TiO₂ powders doped with various transition metals such as Fe, Ni and Cu (Karimipour et al. 2011; Kokil et al. 2011; You et al. 2009). To our best knowledge, the synthesis of Cu-doped TiO₂ via sonochemical process with post thermal treatment has not been available in the literatures.

In the present work, an attempt was carried out to synthesize Cu-doped TiO₂ nanopowders by sonochemical process via a precursor solution of titanium isopropoxide and copper nitrate trihydrate. The effects of calcination temperatures and different Cu dopant content on their physical properties and microstructure were investigated.

Appropriate amounts of titanium (IV) isopropoxide ($C_{12}H_{28}O_4Ti$, Sigma-Aldrich), copper nitrate trihydrate ($Cu(NO_3)_2 \cdot 3H_2O$, Sigma-Aldrich) and sodium hydroxide anhydrous pellets (NaOH) in the presence of polyvinyl alcohol (PVA, Sigma-Aldrich) was used as starting precursor. The Cu doping concentration was varied from 0.1- 0.5 W%. NaOH was added drop-wise to solution until pH became 11-12. The sonication of solution was performed by a Sonics Model VCX 750 until the completely precipitated product was reached. After it was cooled down to room temperature, the precipitates were washed with deionized water and centrifuged at 5,000 rpm for 5 min. The powders were washed several times until it became neutral. Finally, the as-precipitated powders were dried at $100^\circ C$ for 12 h and calcined at different temperature range of $500-1000^\circ C$ for 2 h. The corresponding diagram of synthesis processes is schematically illustrated in Figure 1.

The powder X-ray diffraction (XRD) patterns of the samples were measured by PANalytical diffractometer (X'Pert PRO MPD model pw 3040/60) using $Cu K_\alpha$ ($\lambda = 0.154$ nm) irradiation at a scanning rate (2θ) of $0.02^\circ s^{-1}$ and a 2θ range of $10-60^\circ$ which operated at 40 kV and 30 mA. The morphology of the prepared samples was analyzed using scanning electron microscope (SEM, JEOL JSM-6510). Chemical bonding of the composites was characterized by Fourier transform infrared spectroscopy (FTIR) carried out in the range of $400-4,000$ cm^{-1} in the transmittance mode.

The XRD patterns of 2% Cu-doped TiO_2 powders calcined at different temperatures for 2 h are shown in Figure 2. A noticeable diffraction peak positioned at $2\theta = 25.5^\circ$, which is observed on the spectra of as-synthesized products and the powders calcined at $500^\circ C$ attribute to (101) orientation plane of anatase- TiO_2 . This result indicated that the as-synthesized powder in anatase phase of TiO_2 can be obtained by single step sonochemical process. The possible mechanism for the formation of TiO_2 by sonochemical process is proposed.

At the beginning, dissolved titanium isopropoxide in deionized water under sonication undergoes hydrolysis and condensation process to form hydrolyzed alcoxides, which have great amount of functional hydroxyl groups. Meanwhile, rapid collision driven by strong ultrasound energy can generate localized high temperature area, which can accelerate the condensation reactions of hydroxyl groups to produce the nucleation of fine spherical nanoparticles of TiO_2 (Yu et al. 2009). As the calcinations temperature elevates to $600^\circ C$, the main anatase peak is not detected but new distinct peaks are observed due to rapid phase transformation of TiO_2 at about $600^\circ C$ (Xin et al. 2008). The XRD peak located at 24.7° is indexed to $CuTiO_3$ phase (Truaistaru et al. 2011), meanwhile the observable peaks at 44.6° and 48.9° are assigned to R(210) and A(200), respectively. The other two broad peaks at about 29.4° and 33.2° could be originated from the metastable oxide of Cu and Ti. These features imply the existence of bi-crystalline structure of TiO_2 and the compound oxide of Cu and Ti arises at this temperature.

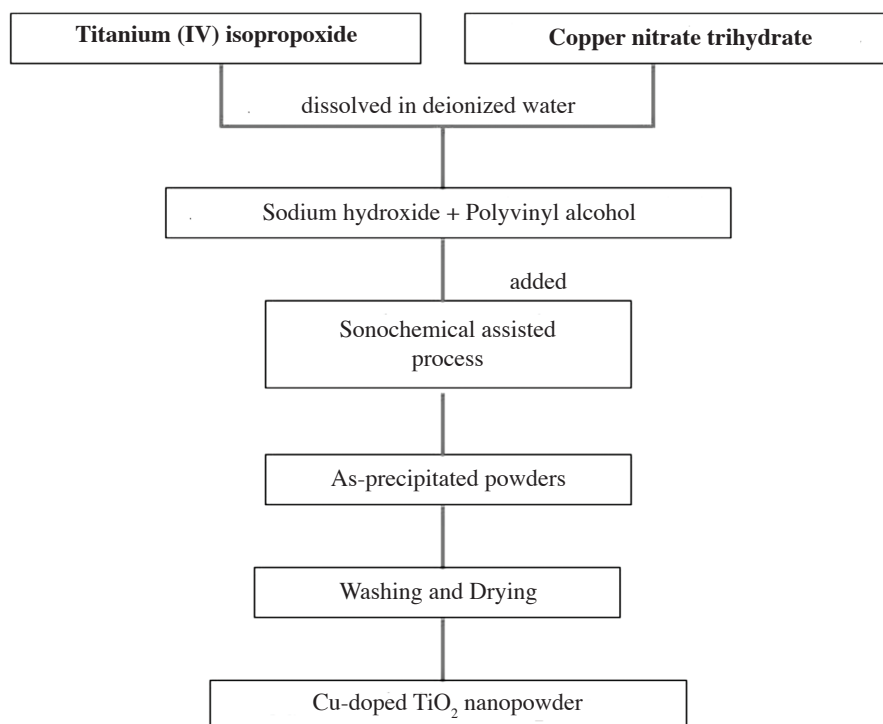


FIGURE 1. Flow chart of the sonochemical process

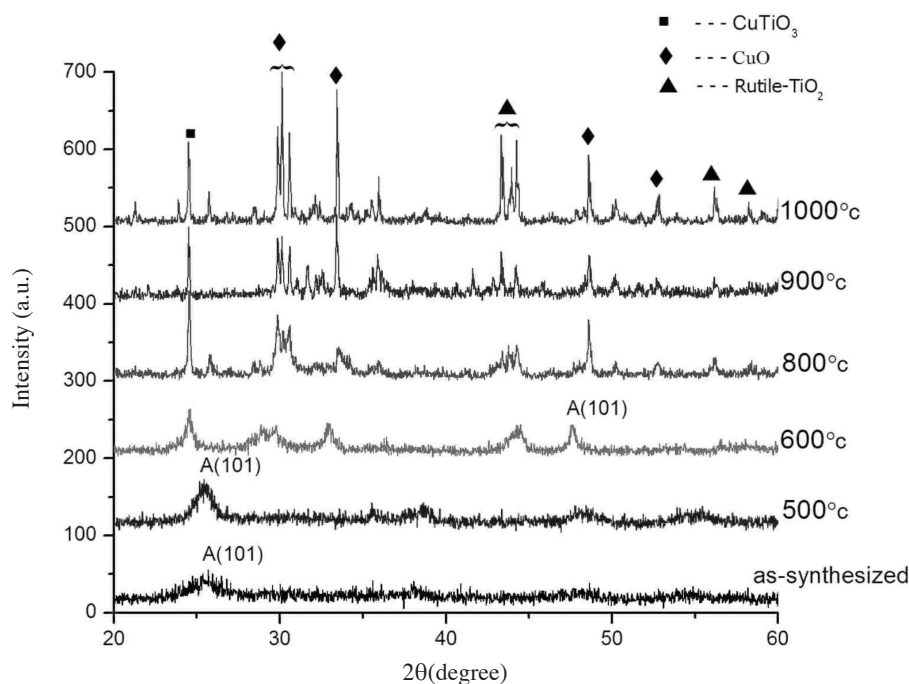


FIGURE 2. The XRD patterns of the 2% Cu-doped TiO_2 calcined at different temperatures

As calcinations temperature increases from this point up to 1000°C , several prominent XRD patterns are detected. The characteristic peaks of CuTiO_3 , CuO (Wang et al. 2009) and rutile- TiO_2 are well indexed by solid square, solid diamond and solid triangle, respectively, showing that the formation of crystalline CuO can be obtained after calcinations at higher temperature of $800\text{--}1000^\circ\text{C}$. Besides, all indexed XRD peak intensities drastically increase with increasing calcinations temperature, reflecting the better crystallization of the oxide compounds with grater grain size. The average crystallite size of nanopowders can be calculated from the full-width at half maximum (FWHM) by well-known Scherrer's formula expressed as:

$$D = \frac{K\lambda}{\beta \cos \theta}, \quad (1)$$

where D is the grain size, K is the shape factor, λ is the X-ray wavelength of $\text{Cu } K_\alpha$ (0.154 nm), β is the full-width at half maximum (FWHM) and θ is the Bragg angle. The (101) peak is used for anatase as the temperature is below 600°C . Meanwhile, as the calcinations temperature is above 600°C , the strongest peak of CuTiO_3 was used for the calculation. The temperature-dependent grain size of Cu-doped TiO_2 synthesized by sonochemical-assisted route is illustrated in Figure 4.

By calculation, the smallest crystallite size of $\sim 10 \text{ nm}$ was obtained from as-synthesized product via sonochemical process of titanium (IV) isopropoxide in the base solution of pH 10-12 and drying at 100°C . At higher calcinations temperatures, the crystallites became larger in size, which can be attributed to the thermally promoted crystallite growth. The size of the anatase crystallites increases from

10 to 16.5 nm when the temperature is raised to 500°C . As the temperature elevates from $500\text{--}900^\circ\text{C}$, the grain size of the powder greatly increases to $\sim 180 \text{ nm}$ with increasing temperature and no further increment in grain size was noticed beyond 900°C . This critical feature may come from the better formation of CuO at this temperature range accompanying the increase in peak intensity of CuO at $800\text{--}1000^\circ\text{C}$ that could quench the grain growth of CuTiO_3 phase. The same manner of decreasing crystal grain size at elevated temperature is agreeable to previous research work conducted by González-Reyes et.al (2010) who reported on the reduction in crystalline size of anatase- TiO_2 beyond 700°C due to phase transformation anatase-to-rutile. In this case, the CuTiO_3 phase shows quite different behavior in which the formation of Cu-Ti oxide phase is somewhat larger than that of anatase phase of TiO_2 . XRD patterns of Cu-doped TiO_2 nanopowders with Cu doping contents of 2% and 3% prepared by sonochemical process and calcined at 900°C are represented in Figure 3. It can be seen that the characteristic peaks of CuTiO_3 and CuO become stronger and more intense with increasing Cu content, suggesting that Cu dopant could promote the better formation of Cu-based oxides.

The SEM images of 2% Cu-doped TiO_2 nanopowders calcined at different temperature are shown in Figure 5. It can be clearly seen that the microstructures of the powders are strongly affected by calcinations temperature. The image of as-synthesized powders as shown in Figure 5(a) is in irregular structure comprising small granular clusters. In temperature range of $500\text{--}600^\circ\text{C}$, the corresponding images disclose the agglomeration of the nanoparticles of the size less than 50 nm . These SEM results are in good

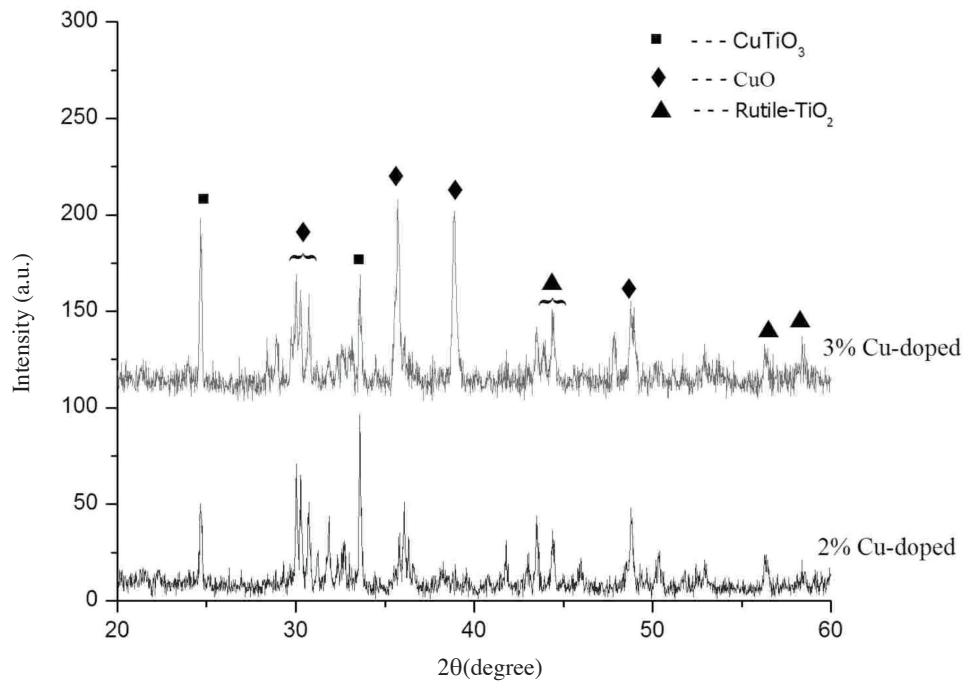


FIGURE 3. The XRD patterns of Cu-doped TiO₂ with different Cu contents calcined at 900°C

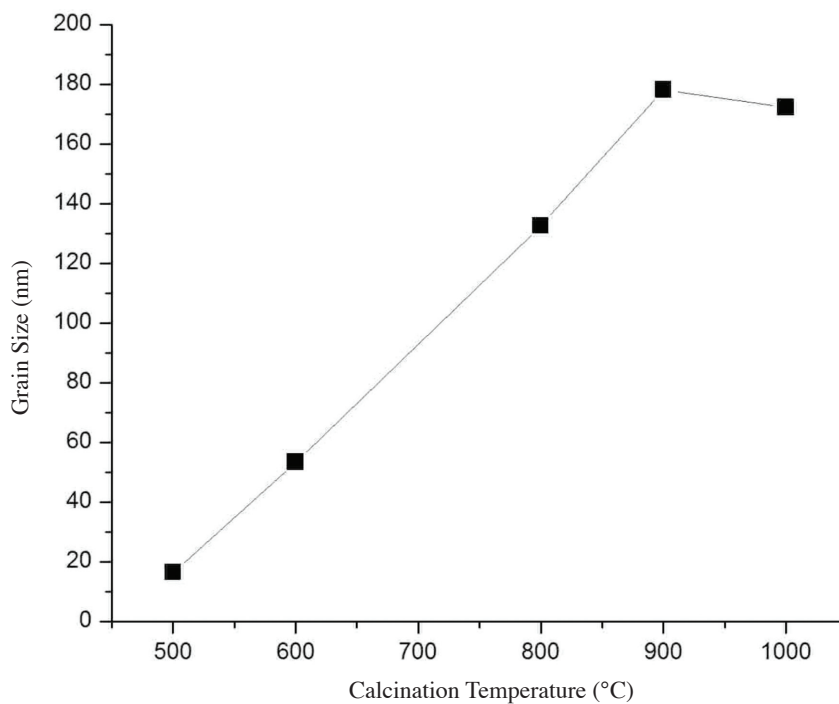


FIGURE 4. The grain size of Cu-doped TiO₂ synthesized by sonochemical-assisted process

agreement with the results interpreted from XRD patterns. As temperature ascends to 800°C, the microstructure of the powders as seen in Figure 5(d) dramatically change and transforms to uniform rectangle rod-like structures with average length greater than 500 nm. Further increasing temperature results to the bigger size of rod-like structure and the formation of platelet shape structure as the

temperature elevates to 1000°C. The SEM results of the samples calcined at high temperature coincidentally affirm the phase transformation of Cu-TiO₂, which is in good agreement to XRD results.

FT-IR measurements of as-prepared powders, powders calcined at 600°C and 1000°C were carried out in the range of 400- 4000 cm⁻¹ and the corresponding results are

shown in Figure 6. The chemical bonding of the powders was scrutinized by correlating the developed peaks in the spectrum to the vibration or stretching of various functional groups. The broad band situated at 3400 cm^{-1} and 1600 cm^{-1} , which are observable in as-prepared powders, are attributed to the stretching and bending vibration of O-H group due to absorbed water molecules, respectively (Li et al. 2005). These two bands are not detected on the spectra of calcined powders due to dehydration during calcinations. The absorption band at 1380 cm^{-1} , that is attributed to the existence of nitrate group can only be observed in as-synthesized sample, suggesting the complete removal of this functional group can be obtained after calcinations process. For the samples calcined at certain temperature, the appearance of new bands below 1000 cm^{-1} are observed.

These bands are associated to the stretching mode of Cu-O and Ti-O (Wang et al. 2009; Yan et al. 2004).

Figure 7 shows the absorption spectra in the wavelength range of 200-700 nm of as-prepared Cu-doped TiO_2 powders and the powders calcined at 500°C and 700°C for 2 h. It can be seen that the enhancement in optical absorption was indicated after the calcinations at high temperature. The strong absorption spectra in range of 200-300 nm with corresponding photon energy of 3.2 eV is due to typical bandgap of TiO_2 . Comparing to as-synthesized sample, the enhancement of absorption spectra in UV and the significant increase of red-shift toward the visible range from 300-700 nm occurred in the raising of temperature at 500°C and 700°C because of the coverage of CuO spectra in UV and visible region (Colon et al. 2006).

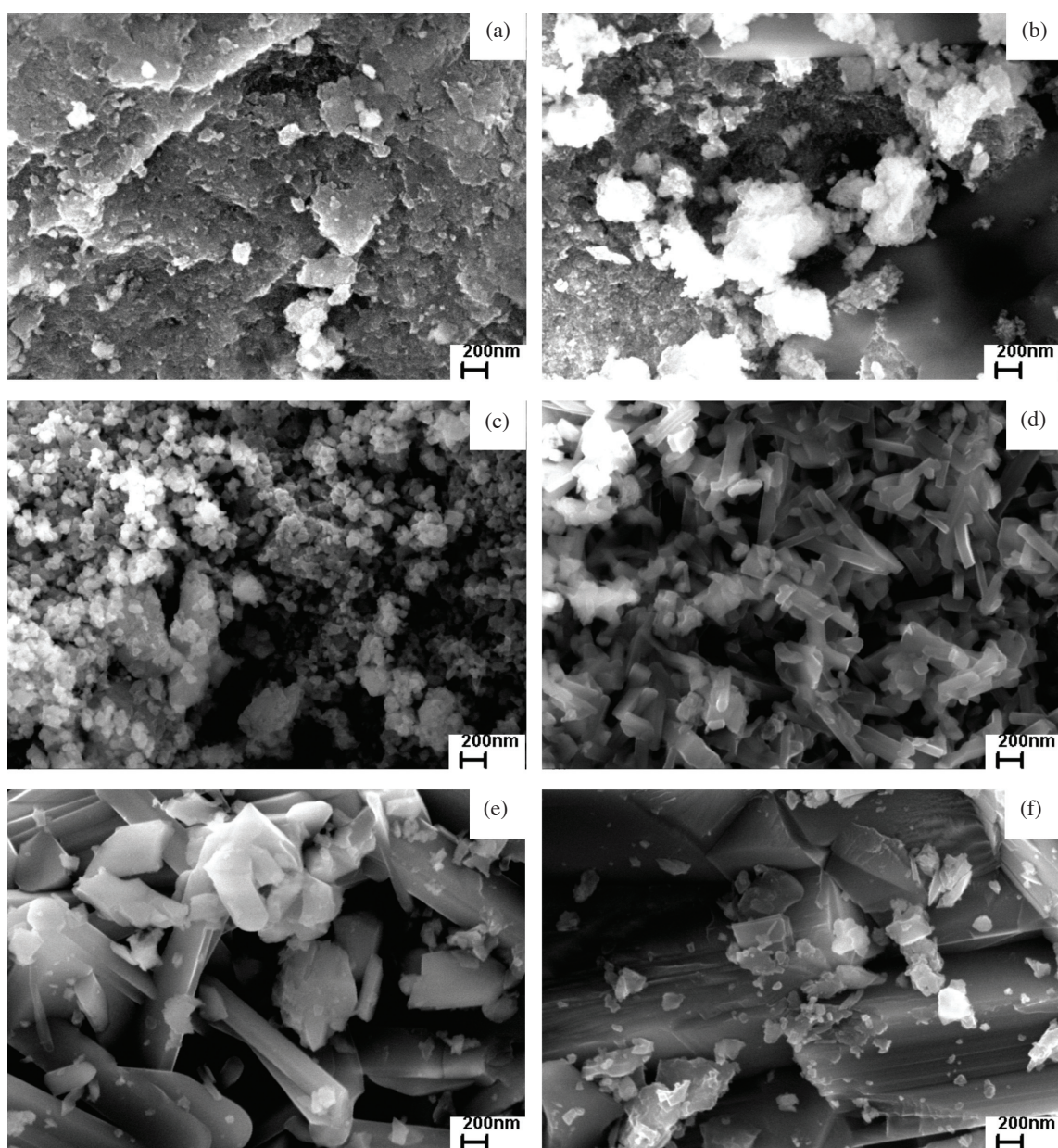


FIGURE 5. SEM images of (a) as-prepared Cu-doped TiO_2 , calcined at (b) 500°C , (c) 600°C , (d) 800°C , (e) 900°C and (f) 1000°C

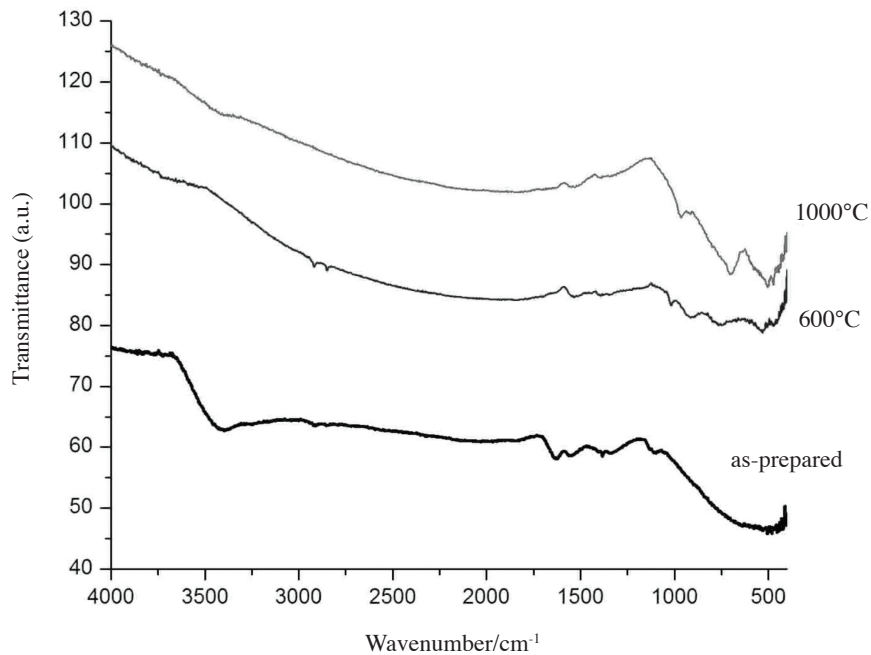


FIGURE 6. The FTIR spectra of the 2% Cu-doped TiO_2 calcined at different temperatures

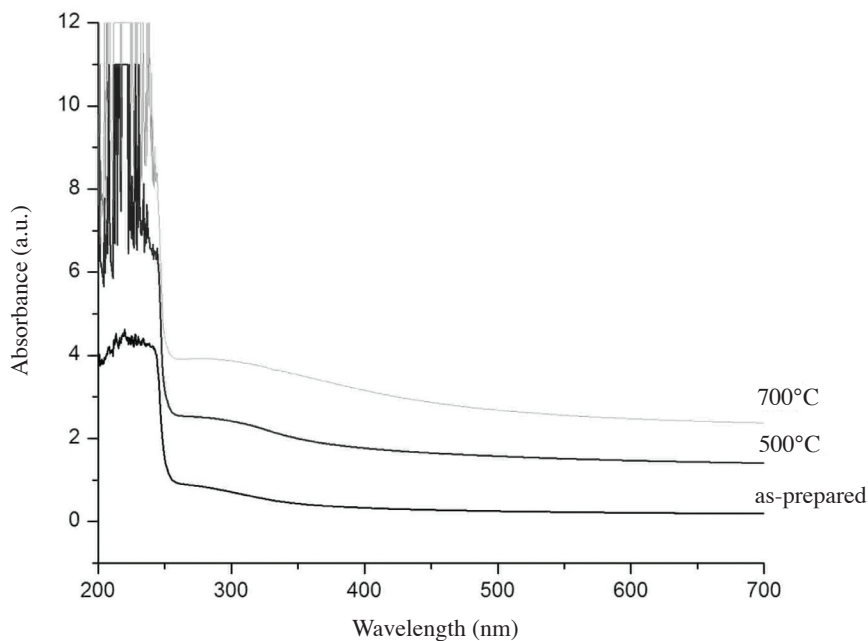


FIGURE 7. The absorption spectra of the 2% Cu-doped TiO_2 calcined at different temperatures

This result implies that the incorporation of Cu additive can effectively enhance the visible response of TiO_2 .

CONCLUSION

In summary, Cu-doped TiO_2 nanopowders were prepared by sonochemical-assisted and calcinations process in temperature range of 500-1000°C. The characterizations of the powders were conducted and the results revealed that as-synthesized powders has an anatase phase of TiO_2 . It was

further acknowledged that the calcinations temperature and the incorporation of Cu dopant have strong influence on physical and optical properties of the powders. The obvious transformation of anatase to rutile phase and the existence of Cu-based oxide were initiated at around 600°C. Further increasing temperature can significantly ameliorate the crystallinity and grain size of all oxide compounds. Their optical absorption results suggested that Cu dopant could significantly improve the optical absorption properties of TiO_2 .

ACKNOWLEDGEMENTS

This work has been partially supported by the National Nanotechnology Center (NANOTEC), NSTDA, Ministry of Science and Technology, Thailand, through its program of Center of Excellence Network. Authors gratefully acknowledge the support from College of Nanotechnology, King Mongkut's Institute of Technology Ladkrabang (KMIL) and Thai Microelectronics Center (TMEC). This work was financially supported by KMIL research fund.

REFERENCES

- Arami, H., Mazloumi, M., Khalifehzadeh, R. & Sadmezhaad, S.K. 2001. Sonochemical preparation of TiO₂ nanoparticles. *Materials Letters* 61: 4559-4561.
- Colon, G., Maicu, M., Hidalgo, M.C. & Navio, J.A. 2006. Cu-doped TiO₂ system with improved photocatalytic activity. *Applied Catalysis B: Environmental* 67: 41-51.
- Deng, C., Hu, H., Ge, X., Han, C., Zhao, D. & Shao, G. 2011. One-pot sonochemical fabrication of hierarchical hollow CuO submicrospheres. *Ultrasonics Sonochemistry* 18: 932-937.
- Gong, D., Grimes, C.A., Varghese, O.K., Hu, W.C., Singh, R.S., Chen, Z. & Dickey, E.C. 2001. Titanium oxide nanotube arrays prepared by anodic oxidation. *Journal of Materials Research* 16: 3331-3334.
- Gonzalez-Reyes, L., Hernandez-Perez, I., Diaz-Barriga Arceo, L., Dorantes-Rosales, H., Arce-Estrada, E., Suarez-Parra, R. & Cruz-Rivera, J.J. 2010. Temperature effects during Ostwald ripening on structural and bandgap properties of TiO₂ nanoparticles prepared by sonochemical synthesis. *Materials Science and Engineering B* 175: 9-13.
- Jitputti, J., Pavasupree, S., Suzuki, Y. & Yoshikawa, S. 2007. Synthesis and photocatalytic activity for water-splitting reaction of nanocrystalline mesoporous Titania prepared by hydrothermal method. *Journal of Solid State Chemistry* 180: 1743-1749.
- Karimipour, M., Wikberg, J.M., Kapaklis, V., Shahtahmasebi, N., Abad, M.R.R., Yeganeh, M., Bagheri-Mohagheghi, M.M. & Svedlindh, P. 2011. Nanoparticles of Ni/ NiO embedded in TiO₂ synthesized by the complex-polymer sol-gel method. *Physica Scripta* 84: 1-5.
- Kasuga, T., Hiramatsu, M., Hoson, A., Sekino, T. & Niihara, K. 1999. Titania nanotubes prepared by chemical processing. *Advanced Materials* 11(15): 1307-1311.
- Kokil, P., Senthilkumar, V. & Nazeer, K.P. 2011. Preparation and photo catalytic activity of Fe³⁺ doped TiO₂ nanoparticles. *Archives of Physics Research* 2(1): 246-253.
- Li, D. & Xia, Y. 2003. Fabrication of Titania nanofibers by electrospinning. *Nano Letters* 3(4): 555-560.
- Li, Z., Hou, B., Xu, Y., Wu, D., Sun, Y., Hu, W. & Deng, F. 2005. Comparative study of sol-gel-hydrothermal and sol-gel synthesis of Titania-Silica composite nanoparticles. *Journal of Solid State Chemistry* 178(5): 1395-1405.
- Truaistaru, G.A., Covaliu, C.I., Opear, O., Matei, V., Cursaru, D.L., Jitaru, I. & Matel, D. 2011. MTiO₃ (M=Cu,Ni) as catalysts in toluene oxidation. *Revista De Chimie* 62(8): 773-776.
- Viana, M.M., Soares, V.F. & Mohallem, N.D.S. 2010. Synthesis and characterization of TiO₂ nanoparticles. *Ceramics International* 36: 2047-2053.
- Wang, D., Zhang, J., Luo, Q., Li, X., Duan, Y. & An, J. 2009. Characterization and photocatalytic activity of poly (3-hexylthiophene)-modified TiO₂ for degradation of methyl orange under visible light. *Journal of Hazardous Materials* 169: 546-550.
- Wang, S., Xu, H., Qian, L., Jia, X., Wang, J., Liu, Y. & Tang, W. 2009. CTAB-assisted synthesis and photocatalytic property of CuO hollow microspheres. *Journal Solid State Chemistry* 182: 1088-1093.
- Xin, B., Wang, P., Ding, D., Liu, J., Ren, Z. & Fu, H. 2008. Effect of surface species in Cu-TiO₂ Photocatalytic activity. *Applied Surface Science* 254: 2569-2574.
- Yan, X., He, J., Evans, D.G., Zhu, Y. & Duan, X. 2004. Preparation characterization and photocatalytic activity of TiO₂ formed from a mesoporous precursor. *Journal of Porous Materials* 11(3): 131-139.
- Yoo, S., Akbar, S.A. & Sandhage, K.H. 2004. Nanocarving of blank Titania crystals into oriented arrays of single-crystal nanofiber via reaction with hydrogen-bearing gas. *Advanced Materials* 16: 260-264.
- You, M., Kim, T.G. & Sung, Y.M. 2009. Synthesis of Cu-doped TiO₂ nanorods with various aspect ratios and dopant concentrations. *Crystal Growth & Design* 10(2): 983-987.
- Yu, C., Yu, J.C. & Chan, M. 2009. Sonochemical fabrication of mesoporous titanium dioxide microspheres. *Journal of Solid State Chemistry* 182: 1061-1069.
- Yu, J., Hai, Y. & Jaroniec, M. 2011. Photocatalytic hydrogen production over CuO- modified Titania. *Journal of Colloid and Interface Science* 357: 223-228.
- Narongdet Wongpisutpaisan*, Naratip Vittayakorn & Wisanu Pecharapa
College of Nanotechnology
King Mongkut's Institute of Technology Ladkrabang
Chalongkrung Rd., Ladkrabang
Bangkok 10520
Thailand
- Naratip Vittayakorn
Department of Chemistry
Faculty of Science
King Mongkut's Institute of Technology Ladkrabang
Chalongkrung Rd., Ladkrabang
Bangkok, 10520
Thailand
- Anucha Ruangphanit
Thai Microelectronics Center
Wangtakien District, Amphur Muang
Chachoengsao, 24000
Thailand
- Wisanu Pecharapa
ThEP Center, CHE
328 Si Ayutthaya Rd.
Bangkok 10400
Thailand

*Corresponding author; email: narongdet.wo@gmail.com

Received: 7 January 2012

Accepted: 21 May 2012